



## Flutter and response of composite wind turbine blade with bending-torsional coupling

Tingrui Liu

College of Mechanical & Electronic Engineering, Shandong University of Science & Technology, Qingdao, China

---

### ABSTRACT

*In this study, flutter and aeroelastic responses of rotor blade with bending-torsional coupling have been investigated for composite thin-walled structure called 'integration line equation closed-section'. The aerodynamic models adopted here are a simple aerodynamic model used for classical flutter and a reduced nonlinear aerodynamic model suitable for constant pitch motion for stall flutter, which are used in order to investigate quickly parameters that influence the behavior of the aeroelastic system. The coupled partial differential structural equation are solved by discretization, with time responses investigated.*

**Keywords:** Classical flutter; Stall flutter; Bending-torsional Coupling; Discretization

---

### INTRODUCTION

Although stability of classical flutter has generally not been a driving issue in utility-scale design, one case in which classical flutter was observed involved a high-speed rotating blade in pitch excitation process. However, with the advent of large wind turbine fitted with relatively slender blades, classical flutter may become a more important design consideration. In addition, innovative blade designs involving the use of aeroelastic tailoring, wherein the blade twists as it bends under the action of aerodynamic loads to shed load resulting from wind turbulence, may increase the blade's proclivity for flutter[1].

The analysis of classical flutter in wind turbines necessitates the use of unsteady aerodynamics [2]. For horizontal axis wind turbines (HAWT) there are two interconnected sources of unsteady aerodynamics. The technique modified for the aeroelastic analysis of a HAWT blade was developed by Theodorsen[3]. Most of the literature of classical flutter focused on the helicopter blades. Chaviaropoulos[4] investigated classical flutter of 2-D section of wind turbine blade on the non-coupling condition. However the aerodynamics of a HAWT system, during catastrophic aeroelastic phenomena, may involve highly separated flows. The nonlinear blade theory for rotating systems has far surpassed what the classical flutter has revealed. So stall flutter should be investigated. Ren[5]adopts a structural equation based on a composite thin-walled beam model with bending-twist coupling, and analyze nonlinear aeroelastic stability for stall flutter. The author has made a literature survey in the subject matter on rotating thin-walled structure (not blade section) systems without structural damping and investigated the nonlinear aeroelastic stability based on linearization in another paper [6]. As for the partial differential equations, which represent the dynamic behavior of wind turbine blade, a radial basis function procedure [7] and Galerkin method [5] are used to transform partial differential equations into a discrete eigenvalue problem.

In this paper, flutter and responses under the circumferentially asymmetric stiffness (CAS) situation of slender composite blade with thin-walled closed cross section are investigated. A number of researchers have developed the numerous solution methods to analyze the vibration problems of composite beams in recent 30 years, especially in the development of analytical expressions for extension-twist coupling and bending-twist coupling. Here a blade

section structural model of coupled partial differential equations is applied based on composite beam theories [8-9]. This model includes the variation of shear modulus in different walls of the cross section in the warping function and transverse shear related couplings. However, restrained warping effects are not included in the model. Flutter and responses of bending-torsional coupling blade integrated with structural damping are analyzed, with influences of ply angles investigated. In this paper, a simple aerodynamic model used for classical flutter and a reduced nonlinear aerodynamic model suitable for constant pitch motion for stall flutter are used in order to investigate quickly a wide range of parameters that control the behavior of the aeroelastic system.

2. Analytical model

2.1 Structural model

Considering the closed-sections of symmetric slender thin-walled composite blade shown in figure 1(a)-(b), the length of the blade is  $L$  in  $x$  direction. The cross-sectional dimension, chord length, is  $c$ . The thickness of blade section is denoted by  $h$ , and the radius of curvature of the middle surface by  $r$ . It is assumed that,  $c \ll L$ ,  $h \ll c$ ,  $h \ll r$ .  $\varphi$  represents twist angle of the closed-section, the pitch angle is  $\beta$ , and the wind velocity is denoted by  $U$ . The middle-line of the thin-walled structure called 'integration line equation closed-section' is as follows [10]:

$$y = e[\exp(0.05((1 - \cos \theta_\varphi)^2 + (\sin \theta_\varphi)^2))] + \exp[-0.05((1 - \cos \theta_\varphi)^2 + (\sin \theta_\varphi)^2)) \cos \theta_\varphi], \quad (1a)$$

$$z = e[\exp(0.05((1 - \cos \theta_\varphi)^2 + (\sin \theta_\varphi)^2))] - \exp[-0.05((1 - \cos \theta_\varphi)^2 + (\sin \theta_\varphi)^2)) \sin \theta_\varphi], \quad (1b)$$

where  $e$  denotes 1/4 chord length, and parameter  $\theta_\varphi$  changes from 0 to  $2\pi$ .

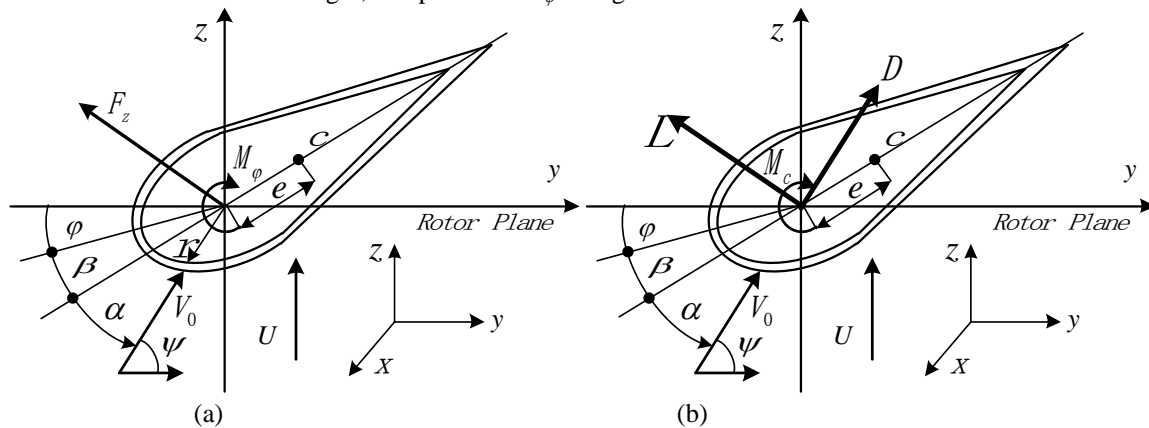


Figure 1. Aerodynamic sectional forces of classical flutter (a) and stall flutter (b)

2.2 Equations of motion for classical flutter

The linear force and torque, illustrated in figure 1(a) and deduced in terms of the lift and moment coefficients for small displacements with the air density  $\rho_a$ , are expressed respectively as follows[4]:

$$F_z = -\rho_a c V_0^2 \pi (\alpha + u'), \quad M_\varphi = -\rho_a c^2 V_0^2 \pi e (\alpha + u'). \quad (2)$$

The equations of free vibration with bending-torsional coupling of anisotropic thin-walled closed-section blade section are derived using a variational asymptotic approach and Hamilton's principle [8-9]. Considering rotation with rotate speed  $\Omega$ , under variable parameters, such as ply angle and wind velocity  $U$ , the following governing equations of motion for blade tip are obtained:

$$[C_{22} + \frac{1}{2} m \Omega^2 K_A^2 (L^2 - x^2)] \varphi'' + C_{23} u''' - m \Omega^2 K_A^2 x \varphi' - I \ddot{\varphi} - m \Omega^2 (K_{m2}^2 - K_{m1}^2) \varphi, \quad (3a)$$

$$= M_\varphi + F_z e \cos(\psi - \varphi - \beta)$$

$$C_{23} \varphi''' + C_{33} u'''' + m \ddot{u} - \frac{1}{2} m \Omega^2 [u''(L^2 - x^2) + u'(-2x)] = F_z \cos(\psi), \quad (3b)$$

where,

$$K_{m1}^2 = \frac{1}{m} \iint \rho_m z^2 dy dz, \quad K_{m2}^2 = \frac{1}{m} \iint \rho_m y^2 dy dz, \quad K_m^2 = K_{m1}^2 + K_{m2}^2, \quad A_0 = \iint dy dz, \quad A_0 K_A^2 = \iint (y^2 + z^2) dy dz.$$

herein,  $m$  is the mass per unit length,  $I$  is the polar mass moment of inertia per unit length about the  $x$  axis.  $u$ ,  $\varphi$  denote flap displacement in direction  $z$  and torsional angle, respectively.  $C_{ij}$  are the cross sectional stiffness. The CAS used here consists of  $[\theta]_{2n}$  in the top side, and  $[-\theta]_{2n}$  in the bottom side, with ply number being 6, ply thickness being  $0.127 \times 10^{-3}$  m.

### 2.3 Equations of motion for stall flutter

Considering constant pitch motion, the nonlinear aerodynamic forces [11], lift ( $L$ ), moment ( $M_c$ ) and drag ( $D$ ), of the cross-section illustrated in figure 1(b), are simplified and reduced to:

$$L = \frac{1}{2} \rho S_L (V_0^2 C_{1L} + V^2 C_{2L}), M_c = \frac{1}{2} \rho S_M (V_0^2 C_{1M} + V^2 C_{2M}), D = \frac{1}{2} \rho c (0.014 V_0^2 + V^2 C_{D2}) \quad (4)$$

where the nonlinear items are:

$$\dot{C}_{1L} + \lambda_L \frac{V_0}{b} C_{1L} = \lambda_L a_{0L} \frac{V_0}{b} \beta, \ddot{C}_{2L} + a_L \frac{V_0}{b} \dot{C}_{2L} + r_L \frac{V_0^2}{b^2} C_{2L} = -r_L \frac{V_0^2}{b^2} \Delta C_L, \dot{C}_{1M} = 0, \quad (5a)$$

$$\ddot{C}_{2M} + a_M \frac{V_0}{b} \dot{C}_{2M} + r_M \frac{V_0^2}{b^2} C_{2M} = -r_M \frac{V_0^2}{b^2} \Delta C_M, \ddot{C}_{D2} + a_D \frac{V_0}{b} \dot{C}_{D2} + r_D \frac{V_0^2}{b^2} C_{D2} = -r_D \frac{V_0^2}{b^2} \Delta C_D; \quad (5b)$$

herein, nonlinear parts in nonlinear items can be expressed as:

$$\Delta C_z = \begin{cases} 0, & \psi \leq \beta + 0.1396 \\ a_{z1}(\psi - \beta - 0.1396), & 0.1396 + \beta < \psi \leq 0.3142 + \beta \\ (a_{z1} + a_{z2})(\psi - \beta) - 0.1396a_{z1} - 0.3142a_{z2}, & \psi > 0.3142 + \beta \end{cases}$$

$$\Delta C_D = -a_{D1}(\psi - \beta) - a_{D2}(\psi - \beta)^2 - a_{D3}(\psi - \beta)^3.$$

where  $z=L$  denotes lift, and  $z=M$  denotes moment respectively. Other related coefficients can be found in reference [6]. So the equations of the stall flutter system are depicted as:

$$[C_{22} + \frac{1}{2} m \Omega^2 K_A^2 (L^2 - x^2)] \varphi'' + C_{23} u''' - m \Omega^2 K_A^2 x \varphi' - I \ddot{\varphi} - m \Omega^2 (K_{m2}^2 - K_{m1}^2) \varphi = \quad (6a)$$

$$M_c + D e \sin(\psi - \beta - \varphi) + L e \cos(\psi - \beta - \varphi),$$

$$C_{23} \varphi''' + C_{33} u'''' + m \ddot{u} - \frac{1}{2} m \Omega^2 [u''(L^2 - x^2) + u'(-2x)] = L \cos(\psi) + D \sin(\psi). \quad (6b)$$

## 3. Reduced equations and structural damping

### 3.1 Reduced equations of motion

Towards the goal of solving the equations as given by Eq. (3), the following steps of discretization will be implemented. The first step consists of representation of displacement functions in the form:

$$\varphi(x, t) = \Phi^T(x) q_\varphi(t), \quad U(x, t) = U^T(x) q_u(t); \quad (7)$$

herein, shape functions are required to satisfy the kinematics and force boundary conditions of the cantilever blade written as:  $\Phi^T(x) = [\varphi_1, \varphi_2, \varphi_3, \varphi_4, \dots, \varphi_N]$ ,  $U^T(x) = [u_1, u_2, u_3, u_4, \dots, u_N]$ , where beam functions  $\varphi_j$  and  $u_j$ , for a cantilevered beam, can be found in reference [12].

Substituting Eq. (7) into Eq.(3) and carrying out the indicated variations and the required integration, result in the equation governing the motion of the system:

$$M_{PN} \ddot{q} + K_{PN} \dot{q} = Q_{PN}, \quad (8)$$

where  $M_{PN}$ ,  $K_{PN}$ , and  $Q_{PN}$  are the  $2N \times 2N$  coefficient matrices, and  $q = [q_\varphi, q_u]^T$ .

### 3.2 Calculation and integrating of structural damping

Modal damping ratio of composite cross-section beam is defined as ratio of dissipated energy to maximum strain energy in the cycle of vibration. Reference [13] studied the local (plate) /global (beam) vibration and damping behavior of composite thin-walled box member subjected to vibratory environment. Based on above theories, reference [5] gave a structural analysis model which can determine the influences of different order modal damping factors for different structural and material parameters. To study the flexural vibration of the slender blade, the paper adopts another method to compute structural damping as depicted in reference [14]. Structural damping can be expressed in terms of an equivalent viscous damping matrix as follows:

$$C_s = a_s K_s = \begin{bmatrix} a_s C_{22} [\Phi^T(x)]'' & a_s C_{23} [U^T(x)]''' \\ a_s C_{23} [\Phi^T(x)]''' & a_s C_{33} [U^T(x)]'''' \end{bmatrix}, \quad a_s = \eta_1 / \omega_1. \quad (9)$$

where  $\omega_1$ , and  $\eta_1$  are the first order natural frequency and the corresponding first order modal damping ratios respectively that can be found in reference [5]. For structural damping computation, a set of composite material parameters are given as, material density  $\rho=1672$  kg/m<sup>3</sup>,  $E_{22}=E_{33}=8.7$  GPa,  $E_{11}=25.8$  GPa,  $\nu_{12}=\nu_{13}=0.34$ ,  $G_{12}=G_{13}=3.5$  Gpa.

Integrating structural damping  $C_s$  into Eq.(8) and carrying out the indicated variations and the required integration resulting in the matrix equations governing the system motion for blade tip, with  $2N \times 2N$  damping matrix  $C_{SN}$ , as follows:

$$M_{PN}\ddot{q} + C_{SN}\dot{q} + K_{PN}q = Q_{PN}, \quad (10)$$

where the added damping matrix  $C_{SN}$  is given as:

$$C_{SN} = \begin{bmatrix} \int a_s C_{22} [\Phi^T(x)]^m \varphi_j dx & \int a_s C_{23} [U^T(x)]^m \varphi_j dx \\ \int a_s C_{23} [\Phi^T(x)]^m u_j dx & \int a_s C_{33} [U^T(x)]^m u_j dx \end{bmatrix}.$$

As for solution of the equations for stall flutter as given by Eq. (6), during the integration in the process of discretization, a strip theory [6], substituting sum operation for integral operation, is used at the right-hand-side terms in Eq. (6). Considering in conjunction with structural discretization equations and aerodynamic equations, and integration with structural damping mentioned above, result in the equations governing the motion of stall flutter:

$$M\ddot{X} + C\dot{X} + KX = Q, \quad (11)$$

where  $X$  is the overall vector of generalized co-ordinates as defined in reference [6].

#### 4. Analysis and results

For this study, some parameters are defined: pitch angle is  $\beta=10^\circ$ , the length of the blade  $L=8.4455\text{m}$ , wind speed  $U=20\text{ m/s}$ , rotate speed  $\Omega=60\text{rpm}$ . The cross sectional stiffness  $C_{ij}$ , are computed and listed in Table 1. The influences of ply angles are investigated and demonstrated.

**Table 1. The cross sectional stiffness (Nm<sup>2</sup>) against ply angles**

Ply angles(°)	0	15	30	45	60	75	90
$C_{22}$	5.2588e5	6.6934e5	9.0369e5	9.0509e5	7.3084e5	5.7973e5	5.2588e5
$C_{23}$	-1.1764e-2	-2.6511e2	-3.1014e2	-1.5919e2	-3.0458e1	9.0908	3.9370e-15
$C_{33}$	1.1491	9.8755e-1	6.8027e-1	4.5931e-1	3.8620e-1	3.8264e-1	3.8749e-1

To determine the responses of the aeroelastic systems in Eqs. (10-11), Simulink can be directly applied. As for eigenvalue problem, take Eq.(10) for example, it will be expressed in state-space form of first order system [6], then numerical simulation for eigenvalue and frequency can be performed.

#### 4.1 Validity of methodology and simulation

To testify validity of the methodology of reduced equations, considering free vibration in Eq.(3) of a cantilever structure, and let  $\Omega=0\text{rpm}$  and  $a_s=0$ , the first five order characteristic natural frequencies of free vibration are computed by comparison with the results of an approximate calculation (AC) method[9]. The approximate solution could be cast as the product of decoupled bending and twisting behavior. The angular frequency can be solved as:

$$\omega^2 = \frac{-(C_{22}m_c\lambda^2 - C_{33}I\lambda^4)}{2m_cI} \pm \frac{\sqrt{(C_{22}m_c\lambda^2 - C_{33}I\lambda^4)^2 + 4m_cI(C_{22}C_{33} - C_{23}^2)\lambda^6}}{2m_cI} \quad (13)$$

where  $\lambda = ik_1$  and  $\lambda = k_2$ ;  $k_1 = (2m + 1)\pi/2L$ , and  $k_2$  is the solution of the equation  $\cos(k_2L)\cosh(K_2L) = -1$ .

Table 2 shows the first five order characteristic frequencies against ply angles from  $0^\circ$  to  $90^\circ$  at interval of  $15^\circ$  solved by methodology in the paper, by comparison with that of AC method. It is obvious that the results both are quite identical.

**Table 2. The first five order characteristic frequencies(Hz) against ply angles**

Ply angles(°)		0	15	30	45	60	75	90
1 <sup>st</sup> frequency	Present	0.0333	0.0298	0.0242	0.0206	0.0193	0.0192	0.0193
	AC	0.0234	0.0205	0.0165	0.0143	0.0135	0.0135	0.0136
2 <sup>nd</sup> frequency	Present	0.2087	0.1840	0.1488	0.1283	0.1208	0.1204	0.1211
	AC	0.2103	0.1843	0.1486	0.1289	0.1217	0.1214	0.1221
3 <sup>rd</sup> frequency	Present	0.5844	0.5192	0.4215	0.3608	0.3384	0.3372	0.3394
	AC	0.5843	0.5120	0.4129	0.3580	0.3382	0.3371	0.3393
4 <sup>th</sup> frequency	Present	1.1452	1.0137	0.8219	0.7055	0.6630	0.6607	0.6650
	AC	1.1452	1.0036	0.8093	0.7016	0.6628	0.6607	0.6650
5 <sup>th</sup> frequency	Present	1.8930	1.6982	1.3868	1.1748	1.0964	1.0923	1.0993
	AC	1.8930	1.6590	1.3378	1.1598	1.0957	1.0922	1.0993

To testify simulation validity of the Simulink process of numerical simulation in stall flutter, results of time response of Eq.(11), representing all the responses of all variables including structural displacement variables and aerodynamic variables, are displayed in figure 2(a). It is clear that all variables are stable, which can be affirmed by analysis of system eigenvalues. Figure 2(b) demonstrates the first ten maximum eigenvalues, all values are far less than 0, which obviously shows the system convergence.

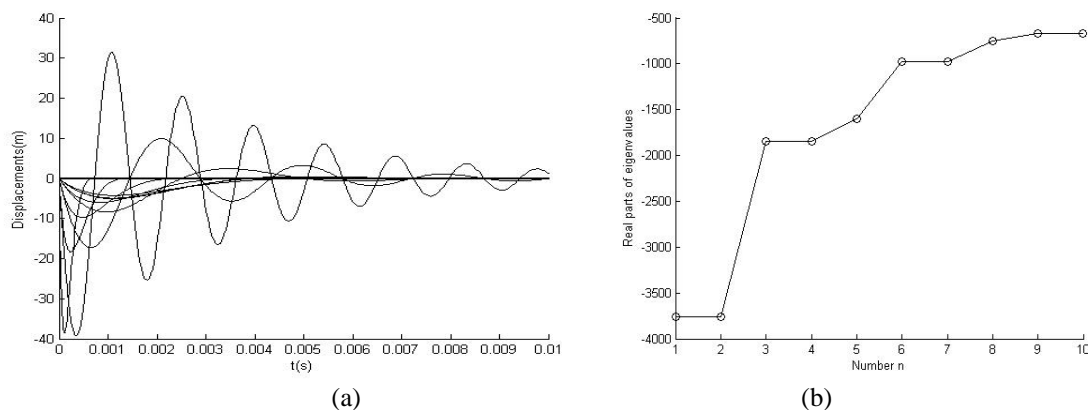


Figure 2. Responses(a) and eigenvalues(b) of stall flutter system.

#### 4.2 The effects of ply angles on stability

Firstly, the influences of ply angles are investigated by responses. Figure 3(a)-(b) show blade tip time responses of the displacements of torsion for classical flutter and stall flutter, respectively. As a rule amplitudes of classical flutter are higher than that of stall flutter, which indicates destructive flutter. For the ply angle of  $45^\circ$ , the trend shows less stability than others. On both sides, stability gradually increases. In ply angle  $15^\circ$ , it is the most stable situation. However in figure 4(a)-(b), it demonstrates the most maximum stability in  $45^\circ$ , and on both sides, stability gradually decreases. In ply angle  $15^\circ$ , it is the most instable situation.

It can be demonstrated that for the given cases, time response amplitudes of the flutter vibration, either for classical flutter or for stall flutter, the change trends of both torsion and flap are consistent, which indicates flutter decreasing. For the given parameters, the system is convergent. It should be stated that the stability rules achieved here are meant to be generalized conclusions for all composite thin-walled blade with different cross-sections and different parameters, in addition to a somewhat data offset of the specific numerical point.

Secondly, the influences of ply angles can be testified by eigenvalue analysis. The aeroelastic system integrated with structural damping has many of  $4N$  eigenvalues or more. It is not easy to distinguish the structural eigenvalues and aerodynamic eigenvalues. So it is unrealistic to prove the structural stability only by eigenvalues. However, for flutter system, real parts of some structural eigenvalues must be zeros, and for the whole aeroelastic system some real parts of eigenvalues must be negative. Furthermore, if the eigenvalues are arranged in order (denotes real parts) from large to small and named in order as the 1<sup>st</sup> eigenvalue, the 2<sup>nd</sup> eigenvalue, the 3<sup>rd</sup> eigenvalue, etc., eigenvalue rules against ply angles might be clarified under conditions of different ply angles for classical flutter and stall flutter.

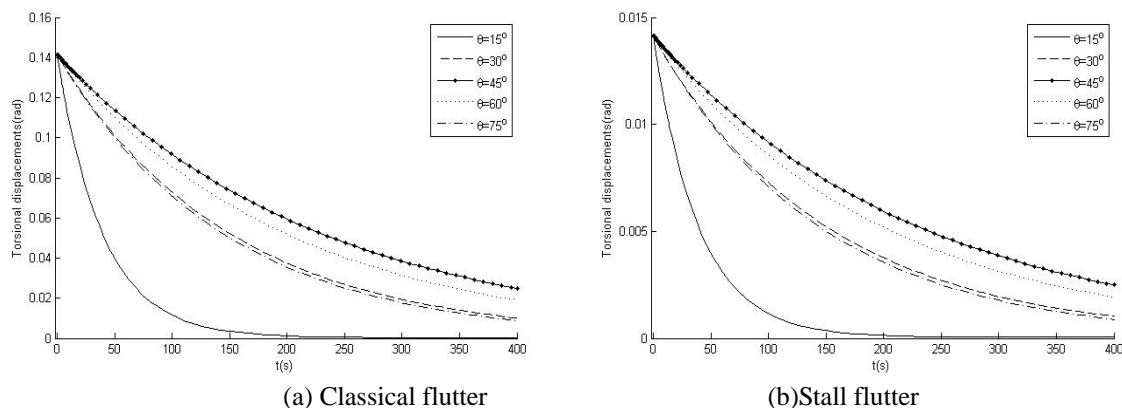


Figure 3. Time responses of torsion against different ply angles.

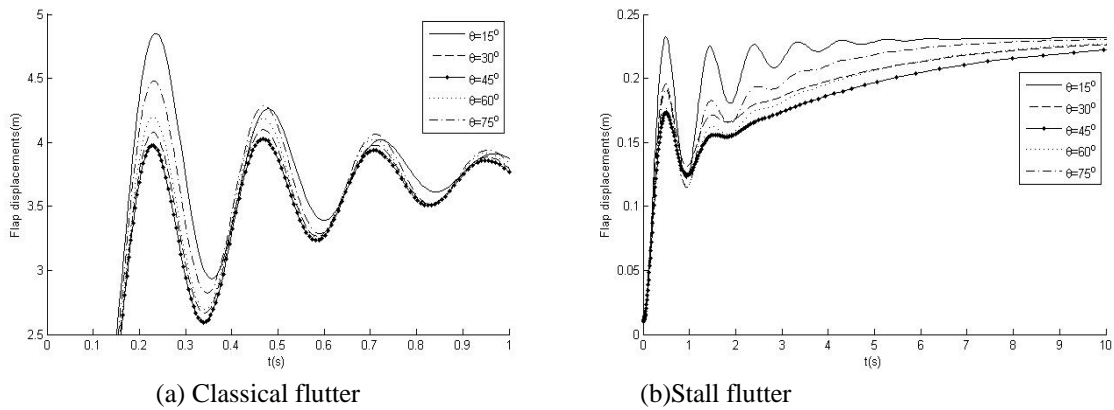


Figure 4. Time responses of flap bending of different ply angles, respectively

Figure 5 show the first four eigenvalues, changing with ply angles from  $15^{\circ}$ ~ $75^{\circ}$  at interval of  $15^{\circ}$ . The results demonstrate that a significant variation in the aeroelastic stability can be achieved against ply angles in general. In addition, the results show that flutter effects are obviously different in ply angle of  $45^{\circ}$  compared with the other ply angles, which are consistent with distribution characteristics of responses shown in figure 3-4. For classical flutter in figure 5(a), the four eigenvalues in ply angles  $15^{\circ}$  are minimum, which shows the most stable state, and in in ply angles  $45^{\circ}$  are the the largest with the most unstable state. For stall flutter in figure 5(b), the four eigenvalues in ply angles  $45^{\circ}$  are almost minimum, which shows the most stable state.

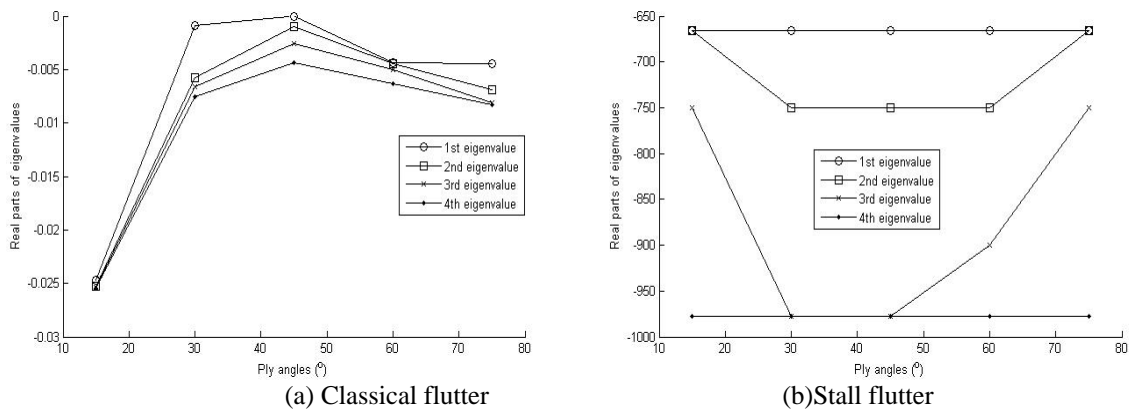


Figure 5. Eigenvalues change with ply angles from  $15^{\circ}$ ~ $75^{\circ}$  at interval of  $15^{\circ}$

## CONCLUSION

Vibration and responses of classical flutter and stall flutter of thin-walled rotor blade with bending-torsional coupling are investigated. Two concluding remarks can be drawn:

- (1) The coupled partial differential equations are reduced to ordinary equations by discretization, and especially structural damping is integrated. Time domain response based on Simulink can be performed to analyze system stability and vibration characteristics of flutter, accompanied by eigenvalue analysis.
- (2) The influences of ply angles of composite blade on stability are investigated. It is obviously demonstrated that different ply angles have different effects on classical flutter and stall flutter.

## Acknowledgment

This work is supported by the Natural Science Foundation of Shandong Provincial of China (ZR2013AM016), and Qunxing Project of Shandong University of Science & Technology (qx2013220).

## REFERENCES

- [1] Don W. Lobitz, *Wind Energy*, Vol.7, pp.211–224, **2004**.
- [2] Leishman J G, *Wind Energy*, Vol.5, pp. 85–132, **2002**.
- [3] Dowell E E, *A Modern Course in Aeroelasticity*, Kluwer: Dordrecht, **1995**.
- [4] Chaviaropoulos P K, Soerensen N N, Hansen M O L, et al, *Wind Energy*, Vol.6, pp. 387–403, **2003**.

- [5] Ren Y S, Liu T R, *Journal of Vibration and Shock*, Vol.32, no.18, 146–152, **2013**.
- [6] Tingrui L, Yongsheng R, *Acta Energiæ Solaris Sinica*, Vol.32, no.1, pp.105–112, **2012**.
- [7] Ming-Hung Hsu, *Advances in Acoustics and Vibration*, Vol.1, pp.1–11, **2011**.
- [8] Armanios E A, Badir A M, *AIAA journal*, Vol.10, pp. 1905–1910, **1995**.
- [9] Dancila D S, Armanios E A, *International Journal of Solids and Structures*, Vol.35, no.23, pp.3105–3119, **1998**.
- [10] Xudon W, Jin C, Wenzhong S, *Chinese Journal of Mechanical Engineering*, Vol.20, no.2, pp.211–213, **2009**.
- [11] Tingrui L, Yongsheng R, Xinghua Y, *Journal of Fluid and Structure*, Vol.42, pp.488–502, **2013**.
- [12] Ramesh C, Inderjit C, *AIAA Journal*, Vol. 29, pp. 657–664, **1992**.
- [13] Ramkumar K, Ganesan N, Kannan R, *European Journal of Mechanics-A/Solids*, Vol.29, pp.253–265, 2010.
- [14] Kumar L R, Datta P K, Prabhakara D L, *International Journal of Mechanical Sciences*, Vol.45, pp.1429–1448, **2003**.